Journal of Applied Sciences

ISSN 1812-5654

Journal of Applied Sciences 7 (1): 72-78, 2007
ISSN 1812-5654

Analyses of MHD Pressure Drop in a Curved Bend for Different Liquid Metals

[1]Kameel Arshad, [2]Muhammad Rafique, [1]Asad Majid and [2]Shahida Jabeen
[1]Pakistan Institute of Engineering and Applied Sciences, P.O. Nilore, Islamabad, Pakistan
[2]Department of Physics, University of Azad Jammu and Kashmir
Muzaffarabad, 13100 Pakistan

Abstract: In this research paper we have analyzed liquid-metal flow in a curved bend in the presence of a magnetic field, which acts in two transverse directions. The magnetic field along the x-axis varied as $B_0(R+x)^{-1}$, while the magnetic field in y-direction is kept constant. The duct has conducting vanadium walls and liquid metal (lithium, sodium and potassium) have been used as a coolant. Magneto hydrodynamic (MHD) equations in three dimensions have been developed in the modified toroidal coordinate system. Then these coupled set of equations are solved by using finite difference techniques and an extended SIMPLER algorithm approach and an estimation of MHD pressure drop has been made for three different liquid metals, namely lithium, sodium and potassium. The results for a curved bend indicate an immense axial MHD pressure drop. The axial MHD pressure drop for three liquid metals, increases for an increase in both kinds of magnetic fields. It has been found that the MHD pressure drop is maximum in the case of sodium and minimum in the case of lithium In this paper a detailed comparative analysis has been carried out to find a suitable fluid for the cooling of high heat flux components of a fusion reactor, which is compatible with liquid metal lithium blanket and can also remove the 5 MW m^{-2} heat flux falling on the limiter or diverter plate. We finally concluded that from MHD pressure drop point of view that liquid lithium is the best choice for cooling of high heat flux components of a fusion reactor

Key words: Magnetic field, liquid-metal flow, magneto hydrodynamic, toroidal coordinate system

INTRODUCTION

Liquid metals and its compounds have been proposed as coolants for fusion reactors. They have also been proposed as coolants for limiters and diverters, the high-heat-flux components of a fusion reactor. Because of its reactivity with liquid metals (lithium, sodium, potassium), water is considered a safety risk (Piet, 1986). It has been observed that liquid metal flows in high-heat-flux components both transverse to the magnetic field and also from a direction parallel to the magnetic field to a direction perpendicular to the magnetic field. The problem of liquid lithium flow in a straight rectangular duct with conducting walls and transverse magnetic field has been looked at by Kim and Abdou (1989). The problem of liquid-metal flow in a curved bend where the magnetic field acts in a single transverse direction to the coolant flow for a straight duct and a curved bend has been looked at by Asad (Majid, 1999). However the MHD pressure drop in the presence of two transverse magnetic fields for different liquid metals (lithium, sodium, potassium) has not been looked at. Knowledge about the MHD pressure drop in the presence of two transverse magnetic fields, one in the x direction and varying as

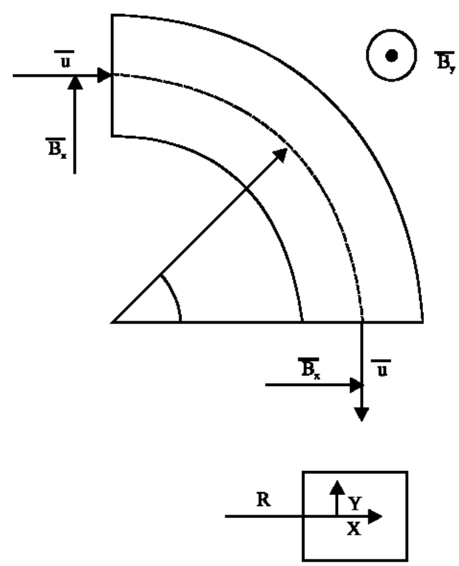

Fig. 1: Geometric configuration of the curved bend

Corresponding Author: Muhammad Rafique, Department of Physics, University of Azad Jammu and Kashmir Muzaffarabad, 13100 Pakistan

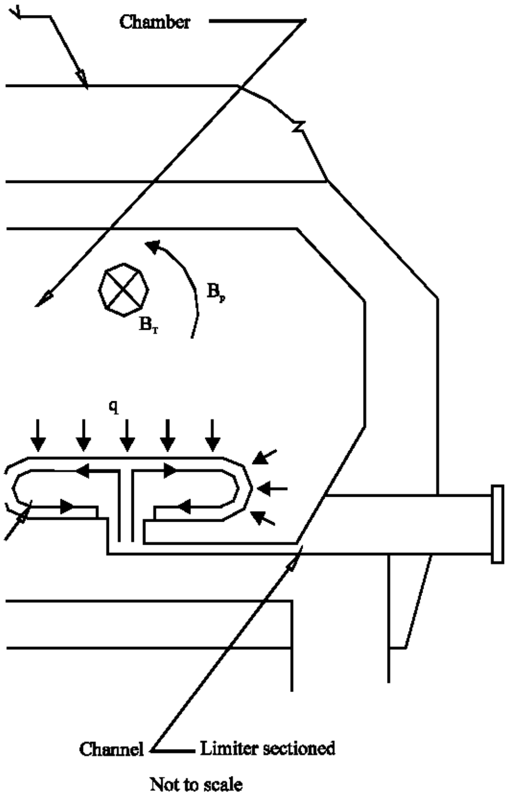

Fig. 2: Geometric configuration of the coolant channel

$B_0(R+x)^{-1}$ (Fig. 1) and the other a constant magnetic field in they direction (Fig. 1), is necessary to accomplish a feasible fusion reactor design. A square-cross-section coolant channel was selected for analysis. This channel represents the cooling channel on the face of a limiter or diverter. The channel analyzed would closely resemble the channel on the leading edge of the limiter or diverter (Baker, 1980). Figure 2 shows the geometric configuration of this channel. The coordinate system can be called a modified toroidal coordinate system (Fig. 1) because the cross section of the torus in modified toroidal coordinate system is rectangular while the cross section of the torus in toroidal coordinate system is circular (Fig. 1).

THE MHD EQUATIONS

The MHD equations, assuming the conditions of steady state, incompressible flow, constant properties, negligible viscous dissipation and negligible induced magnetic field, are expressed in vector from as follows:

Continuity:

$$\nabla.u = 0$$

Momentum:

$$\rho(u.\nabla u) = -\nabla P + \mu\, \nabla.\nabla u + \sigma(-\nabla\phi + u\times B)\times B$$

Ohm's Law:

$$J = \sigma(-\nabla\phi + u\times B)$$

Potential equation:

$$\nabla^2\phi - \nabla.(u\times B) = 0$$

Where

B	=	Magnetic field
u	=	Vectorial velocity
ϕ	=	Electrical potential
P	=	Pressure
ρ	=	Fluid density
σ	=	Electrical conductivity
μ	=	Absolute viscosity
J	=	Electrical current

It has been observed that when liquid metal flows in a duct with conducting walls, the free charge available makes a path through the conducting walls. This current interacts with the magnetic field. If the orientation of the magnetic field is transverse to the flow, then a net force (J X B) develops, which tends to retard the flow and thus gives rise to MHD pressure drop. It can be seen from the momentum equation that in MHD flows in the presence of magnetic field, three kinds of fields affect the flow. They are the pressure field, the potential field and the magnetic field.

The vectorial MHD equations were then expressed in terms of the space variables x, y, θ of the modified toroidal coordinate system, with x representing distance in the radial direction from the duct centerline, y the distance normal to the radial direction and θ the angle around the loop in the axial direction. The differential equations in terms of the space variables x, y and θ and the major radius, are obtained by the use of metric coefficients and are given next (Note that u is the velocity in the x direction, v is the velocity in the y direction and w is the velocity in the axial direction):

Continuity:

$$\frac{1}{R+x}\left[\frac{\partial}{\partial x}((R+x)u)+\frac{\partial}{\partial y}((R+x)v)+\frac{\partial}{\partial \theta}(w)\right]=0,$$

x-momentum:

$$\frac{1}{R+x}\left[\frac{\partial}{\partial x}\left\{(R+x)\rho uu-\mu(R+x)\frac{\partial u}{\partial x}\right\}\right]$$
$$+\frac{1}{R+x}\left[\frac{\partial}{\partial y}\left\{(R+x)\rho vu-\mu(R+x)\frac{\partial u}{\partial y}\right\}\right]$$
$$+\frac{1}{R+x}\left[\frac{\partial}{\partial \theta}\left\{\rho wu-\frac{\mu}{(R+x)}\frac{\partial u}{\partial \theta}\right\}\right]=-\frac{\partial P}{\partial x}+\frac{\rho ww}{(R+x)}$$
$$-\frac{2\mu}{(R+x)(R+x)}\frac{\partial w}{\partial \theta}-\frac{\mu\mu}{(R+x)(R+x)}+\sigma B_\theta wB_x$$
$$-\sigma B_\theta B_\theta u-\sigma B_\theta\frac{\partial \phi}{\partial y}-\sigma uB_yB_y+\sigma B_yB_xv$$
$$+\sigma\frac{B_y}{(R+x)}\frac{\partial \phi}{\partial \theta},$$

y-momentum:

$$\frac{1}{R+x}\left[\frac{\partial}{\partial x}\left\{(R+x)\rho uv-\mu(R+x)\frac{\partial v}{\partial x}\right\}\right]$$
$$+\frac{1}{R+x}\left[\frac{\partial}{\partial y}\left\{(R+x)\rho vv-\mu(R+x)\frac{\partial v}{\partial y}\right\}\right]$$
$$+\frac{1}{R+x}\left[\frac{\partial}{\partial \theta}\left\{\rho wv-\frac{\mu}{(R+x)}\frac{\partial v}{\partial \theta}\right\}\right]=-\frac{\partial P}{\partial y}$$
$$+\sigma B_\theta wB_y-\sigma B_\theta B_\theta v+\sigma B_\theta\frac{\partial \phi}{\partial x}+\sigma uB_yB_x$$
$$-\sigma B_xB_xv-\sigma\frac{B_x}{(R+x)}\frac{\partial \phi}{\partial \theta},$$

θ-momentum:

$$\frac{1}{R+x}\left[\frac{\partial}{\partial x}\left\{(R+x)\rho uw-\mu(R+x)\frac{\partial w}{\partial x}\right\}\right]$$
$$+\frac{1}{R+x}\left[\frac{\partial}{\partial y}\left\{(R+x)\rho vw-\mu(R+x)\frac{\partial w}{\partial y}\right\}\right]$$
$$+\frac{1}{R+x}\left[\frac{\partial}{\partial \theta}\left\{\rho ww-\frac{\mu}{(R+x)}\frac{\partial w}{\partial \theta}\right\}\right]=$$
$$-\frac{1}{R+x}\frac{\partial P}{\partial \theta}-\frac{\rho uw}{(R+x)}+\frac{2\mu}{(R+x)(R+x)}\frac{\partial u}{\partial \theta}$$
$$-\frac{\mu w}{(R+x)(R+x)}+\sigma B_\theta vB_y-\sigma B_yB_yw-$$
$$\sigma B_y\frac{\partial \phi}{\partial x}-\sigma wB_xB_x+\sigma B_\theta B_xu+\sigma B_x\frac{\partial \phi}{\partial y},$$

Potential equation:

$$\frac{1}{R+x}\left[\frac{\partial}{\partial x}\left((R+x)\frac{\partial \phi}{\partial x}\right)+\frac{\partial}{\partial y}\left((R+x)\frac{\partial \phi}{\partial y}\right)\right.$$
$$\left.+\frac{\partial}{\partial \theta}\left(\frac{1}{(R+x)}\frac{\partial \phi}{\partial \theta}\right)\right]$$
$$=-\frac{1}{(R+x)}\left[\frac{\partial}{\partial x}((R+x)(vB_\theta-wB_y))+\frac{\partial}{\partial y}\right.$$
$$\left.((R+x)(wB_x-uB_\theta))+\frac{\partial}{\partial \theta}(uB_y-vB_x)\right]$$

METHOD OF SOLUTION

The differential equations described above were solved using the finite difference techniques described by Patankar, 1980; 1979b; Patankar and Spalding (1970, 1972a, b; 1974a, b; 1978). The new computer code SIMPLMHD (Majid, 1990) was upgraded to incorporate the three different liquid metal properties at 230°C (Holman, 1976; Charles, 1958). This code incorporates the extended SIMPLER method (Majid, 1990) for solving the coupled set of MHD equations.

The discretization equations were developed using the control volume approach. The numerical scheme used was the power law scheme (Patankar, 1980, 1979a, b; Patankar and Spalding, 1970, 1972a, b; 1974a, b; 1978). The potential equation is solved by ordinary finite difference techniques. The final discretization equations, where the magnetic field is assumed to operate in the x-θ plane as well as in the y direction are obtained as follows:

x-momentum:

$$u_p(a_T+a_B+a_N+a_S+a_E+a_W)=a_Tu_T+a_Bu_B$$
$$+a_Nu_N+a_Su_S+a_Eu_E+a_Wu_W+\left[\frac{\rho ww}{(R+x)}\right]\Bigg|_P$$
$$-2\mu\left[\frac{w}{(R+x)}\right]\Bigg|_t\Delta x\Delta y+2\mu\left[\frac{w}{(R+x)}\right]\Bigg|_b\Delta x\Delta y$$
$$-\left[\frac{\mu u}{(R+x)(R+x)}\right]\Bigg|_P\Delta V-\left[P_e-P_w\right]\delta A(x)$$
$$+\left[\sigma B_\theta B_xw\right]_p\Delta V-\left[\sigma B_\theta B_\theta u\right]_p\Delta V-\left[\sigma B_\theta(R+x)\phi\right]_n$$
$$\Delta\theta\Delta x+\left[\sigma B_\theta(R+x)\phi\right]_s\Delta\theta\Delta x-\left[\sigma B_yB_yu\right]_p\Delta V$$
$$+\left[\sigma B_yB_xv\right]_p\Delta V+\left[\sigma B_y\phi\right]_n\Delta x\Delta y-\left[\sigma B_y\phi\right]_S\Delta x\Delta y$$

where

ΔV	=	Volume of control volume
P	=	Location of grid point of interest
n	=	Northern face of control volume
s	=	Southern face of control volume
e	=	Eastern face of control volume
w	=	Western face of control volume
t	=	Top face of control volume
b	=	Bottom face of control volume
W, E	=	Location of the neighboring points in the x direction
S, N	=	Location of the neighboring points in the y direction
B, T	=	Location of the neighboring points in the θ direction
δA (x)	=	Area of the control volume face perpendicular to x-direction and where

$$a_T = D_t A(|P_t|) + [|-F_t, 0|];\ a_B = D_b A(|P_b|) + [|F_b, 0|]$$
$$a_N = D_n A(|P_n|) + [|-F_n, 0|];\ a_S = D_s A(|P_s|) + [|F_s, 0|]$$
$$a_E = D_e A(|P_e|) + [|-F_e, 0|];\ a_W = D_w A(|P_w|) + [|F_w, 0|]$$
$$a_p = a_T + a_B + a_N + a_S + a_E + a_W$$
$$D_t = \frac{\mu}{\left((R+x)d\theta\right)\big|_t}\Delta x\Delta y;\ D_b = \frac{\mu}{\left((R+x)d\theta\right)\big|_b}\Delta x\Delta y$$

$$D_n = \frac{\mu(R+x)\big|_n \Delta x\Delta\theta}{\delta y_n};\ D_s = \frac{\mu(R+x)\big|_s \Delta x\Delta\theta}{\delta y_s}$$
$$D_e = \frac{\mu(R+x)\big|_e \Delta y\Delta\theta}{\delta y_e};\ D_s = \frac{\mu(R+x)\big|_s \Delta x\Delta\theta}{\delta y_s}$$
$$D_e = \frac{\mu(R+x)\big|_e \Delta y\Delta\theta}{\delta y_e};\ D_w = \frac{\mu(R+x)\big|_w \Delta y\Delta\theta}{\delta y_w}$$
$$P_e = \frac{F_e}{D_e};\ P_w = \frac{F_w}{D_w};\ P_n = \frac{F_n}{D_n};\ P_s = \frac{F_s}{D_s};\ P_t = \frac{F_t}{D_t};\ P_b = \frac{F_b}{D_b}$$
$$F_e = (R+x)\rho u\big|_e \Delta y\Delta\theta;\ F_w = (R+x)\rho u\big|_w \Delta y\Delta\theta$$
$$F_n = (R+x)\rho v\big|_n \Delta x\Delta\theta;\ F_s = (R+x)\rho v\big|_s \Delta x\Delta\theta$$
$$F_t = (R+x)\rho w\big|_t \Delta y\Delta x;\ F_b = (R+x)\rho w\big|_b \Delta y\Delta x$$
$$A(|P|) = \left[\left|0, (1-0.1|P|)^5\right|\right]$$

operator $[|C,K|]$ = the greater of Majid (1999)
$\Delta x, \Delta y, \Delta\theta$ = dimensional parameters of the control volume
$w|_b$ = calculation of the w velocity at the corresponding location of the bottom face of the control volume and similarly for others with this notation.

δx, δy, δz = distance between the grid points in the *x*, *y* and *z* directions, respectively.

y-momentum:

$$\begin{aligned}
&w_p(a_T + a_B + a_N + a_S + a_E + a_W) = a_T w_T \\
&+ a_B w_B + a_N w_N + a_S w_S + a_E w_E + a_W w_W \\
&-[P_n - P_s]\delta A(y) - [\sigma B_\theta B_\theta \upsilon]_p \Delta V + [\sigma B_y B_\theta w]_p \\
&\Delta V - [\sigma B_x B_x \upsilon]_p \Delta V + [\sigma B_y B_x u]_p \Delta V + \\
&[\sigma B_\theta (R+x)\phi]_e \Delta\theta\Delta y - [\sigma B_\theta (R+x)\phi]_w \\
&\Delta\theta\Delta y - \sigma\left((B_x\phi|_t)\right)\Delta x\Delta y + \sigma\left((B_x\phi|_b)\right)\Delta x\Delta y
\end{aligned}$$

where the coefficients of the discretization equation and the nomenclature are the same as the coefficients and nomenclature for the x-momentum equation except for the fact that they now pertain to the control volume around the v velocity.

θ-momentum:

$$\begin{aligned}
&w_p(a_T + a_B + a_N + a_S + a_E + a_W) = a_T w_T \\
&+ a_B w_B + a_N w_N + a_S w_S + a_E w_E + a_W w_W \\
&-[P_n - P_s]\delta A(y) - [\sigma B_\theta B_\theta \upsilon]_p \Delta V + [\sigma B_y B_\theta w]_p \\
&\Delta V - [\sigma B_x B_x \upsilon]_p \Delta V + [\sigma B_y B_x u]_p \Delta V + \\
&[\sigma B_\theta (R+x)\phi]_e \Delta\theta\Delta y - [\sigma B_\theta (R+x)\phi]_w \\
&\Delta\theta\Delta y - \sigma\left((B_x\phi|_t)\right)\Delta x\Delta y + \sigma\left((B_x\phi|_b)\right)\Delta x\Delta y
\end{aligned}$$

Where the coefficients of the discretization equation and the nomenclature are the same as the coefficients and nomenclature for the x-momentum equation except for they pertain to the control volume around the w velocity.

Potential equation:

$$\begin{aligned}
&a_P\phi_P = a_E\phi_E + a_W\phi_W + a_N\phi_N + a_S\phi_S + a_T\phi_T \\
&+ a_B\phi_B - \left(((R+x)(vB_\theta - wB_y))\big|_e\right)\Delta y\Delta\theta + \\
&\left(((R+x)(vB_\theta - wB_y))\big|_w\right)\Delta y\Delta\theta + \\
&\left(((R+x)(wB_x - uB_\theta))\big|_n\right)\Delta x\Delta\theta - \\
&\left(((R+x)(wB_x - uB_\theta))\big|_s\right)\Delta x\Delta\theta + \\
&\left((uB_y - vB_x)\big|_t - (uB_y - vB_x)\big|_b\right)\Delta y\Delta x,
\end{aligned}$$

where

$$a_E = \frac{(R+x)|_e}{\delta x_e}\Delta y\Delta\theta \quad a_w = \frac{(R+x)|_w}{\delta x_w}\Delta y\Delta\theta$$

$$a_N = \frac{(R+x)|_n}{\delta x_n}\Delta x\Delta\theta \quad a_S = \frac{(R+x)|_s}{\delta x_s}\Delta x\Delta\theta$$

$$a_T = \frac{1}{(R+x)|_t}\frac{1}{\delta\theta_t}\Delta x\Delta y \quad a_B = \frac{1}{(R+x)|_b}\frac{1}{\delta\theta_b}\Delta x\Delta y$$

$$a_P = a_E + a_W + a_N + a_S + a_T + a_B$$

The definition of various control volume parameters is the same as given for the x-momentum equation, only now they pertain to the control volume around the potential.

The boundary conditions for solving the momentum equations evolve from the no slip condition where the velocities u, v and w are zero at the wall. The boundary condition to solve the potential equation is the thin wall boundary condition where the walls are thin enough that current cannot flow in a direction in which the wall is thin but can flow only in the direction along which walls extend (Majid, 1990).

The significant feature of these analyses was the development of the pressure equation by combining continuity and discretized momentum equations. The final set of equations to be solved consisted of three discretized momentum equations for three velocities u, v and w; one pressure equation and one electric potential equation.

The first step according to the SIMPLER algorithm was to guess a velocity field. An electric potential field was also guessed. The magnetic field was given. The various steps of the SIMPLER algorithm were then followed until a converged velocity field and pressure field were obtained. With the newly achieved converged velocity field and pressure field, the potential equation was solved and a potential field was obtained. With the newly obtained velocity field, pressure field and electric potential field, the whole procedure was repeated; i.e., the various steps of the SIMPLER algorithm were followed where in place of guessed fields newly calculated fields were used. This procedure was repeated until a converged electric potential field along with a velocity field and a pressure field was obtained.

ANALYSIS OF FLOW IN A CURVED BEND

The computer code SIMPLMHD was written, as mentioned earlier in such away that results can be obtained for two geometries, a straight duct and a curved bend, by controlling the major radius R. The exit condition of the flow was considered as fully developed. As the length of the bend under consideration is not sufficient for the flow to become fully developed, the specification of the exit condition needs justification. The justification is that the Peclet number for axial flow is sufficiently large (Peclet number> 100) thus the flow conditions downstream at the exit will not significantly affect the flow conditions upstream at the exit. The assumption of fully developed conditions at the exit will thus not cause any significant error in the analysis. It was assumed that at the inlet, the flow enters with a three dimensional parabolic velocity profile. The assumption in the inlet profile is not expected to drastically effect our calculations as we start measuring the pressure from the plane next to the inlet plane. It has to be noted that the magnetic field force affecting the flow is so strong as compared with the ordinary hydrodynamic forces that the flow takes up the magnetic effects within a very small distance from the inlet. This can be seen from the ordinary hydrodynamic pressure drop, which is only about 400 Pa m^{-1} as compared with the MHD pressure drop, whose minimum value is about 20000 Pa m^{-1} and soars above this value as magnetic field strength is increased. Thus any error because of an inlet profile assumption is expected to be nulled out within the movement of the fluid from the first inlet plane to the second plane in the direction of the flow.

The dimensions of the channel analyzed were 1×1 cm. The bend analyzed had a radius of 5 cm. The magnetic field in the x direction in the case of the curved bend was considered to vary as $B_0(R+x)^{-1}$, as a constant magnetic field in the x direction would violate the Maxwell's equation. The magnetic field in the y direction is considered to be constant. The wall thickness was taken to be 1 mm. The flow was analyzed at a Reynolds number of 5276 for lithium, 13928 for sodium and 16411 for potassium.

The calculation of the pressure gradient (Pascal per meter) in a 5 cm radius bend when magnetic field acts in both x and y directions was performed. The pressure gradient along the curved bend for different values of center line magnetic field and different values of constant magnetic field in y direction is shown in Fig. 3 for lithium. It is observed that pressure gradient increases for an increase in the center line magnetic field and also increases for an increase in the magnetic field in y direction. The pressure gradient along the curved bend for different values of center line magnetic field and different values of constant magnetic field in y direction is shown in Fig. 4 for sodium.

It is observed that pressure gradient increases for an increase in the center line magnetic field and also increases for an increase in the magnetic field in y direction. The pressure gradient along the curved bend

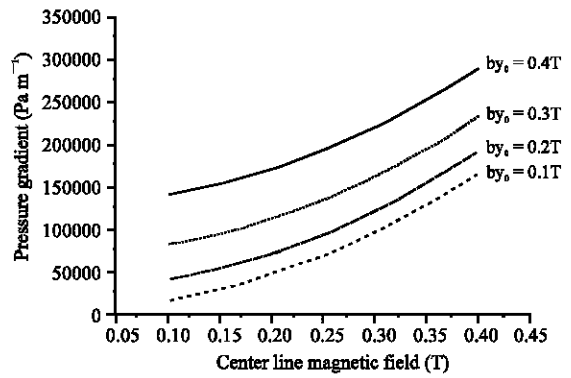

Fig. 3: Lithium with varying by_0 field

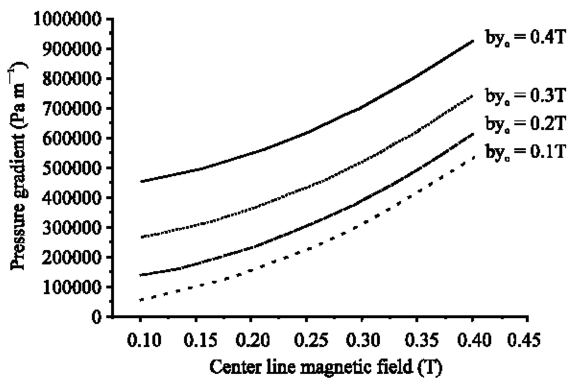

Fig. 4: Sodium with varying by_0 field

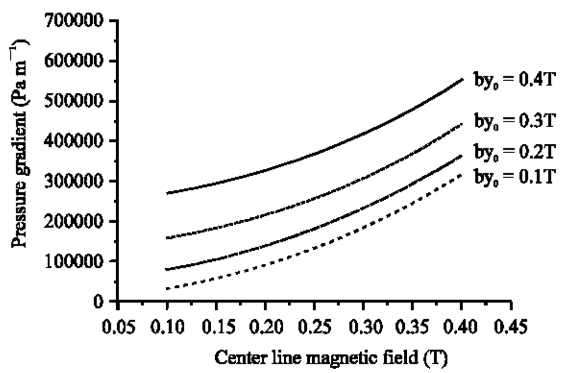

Fig. 5: Potassium with varying by_0 field

for different values of center line magnetic field and different values of constant magnetic field in y direction is shown in Fig. 5 for potassium. It is observed that pressure gradient increases for an increase in the center line magnetic field and also increases for an increase in the magnetic field in they direction. A comparative plot of pressure gradient for three different fluids is shown in Fig. 6. It can be seen very clearly that MHD pressure drop is maximum for sodium and minimum for lithium.

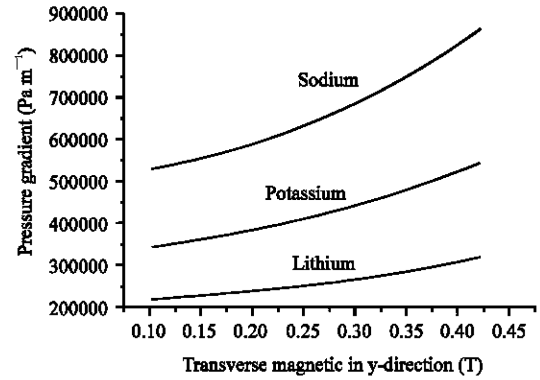

Fig. 6: Comparative plot of pressure gradient for three different fluids

CONCLUSIONS

The purpose of these comparative analyses was to look for a fluid for the cooling of high heat flux components of a fusion reactor, which is compatible with liquid metal lithium blanket and can also remove the 5 MW/m^{-2} heat flux falling on the limiter or diverter plate. Thus a low-pressure system which can allow enhancement of the heat transfer through greater fluid velocities is highly desirable. As higher MHD pressure drop would lead to higher-pressure systems thus a liquid metal which would give rise to lower MHD pressure drop is desirable. Our results however indicate that lithium still remains the liquid metal giving rise to minimum pressure drop as compared with sodium and potassium. We can finally conclude that from MHD pressure drop point of view liquid lithium is the best choice for cooling of high heat flux components of a fusion reactor.

REFERENCES

Baker, C.C., 1980. Starfire, ANL/FPP-80-1, September.

Charles, L.M., 1958. Engineering Materials Handbook. 1st Edn., New York, Toronto, London, McGraw-Hill Book Company, Printed by a staff of Specialists.

Holman, J.P., 1976. Heat Transfer 4th Edn., McGraw-Hill Kogakusha, LTD. Tokyo, 1976.

Kim, C.N. and M.A. Abdou, 1989. Numerical method for fluid heat flow and heat transfer in magneto hydrodynamic Flow. Proc. 10th Topl. Mtg. Technology of Fusion Energy, Salt Lake City Utah.

Majid, A., 1990. Use of Liquid Metals for Cooling High Heat Flux Components of a Fusion Reactor. Ph.D Thesis, University of California, Los Angeles.

Majid, A., 1999. Magneto hydrodynamic pressure drop in a straight duct and a curved bend in the presence of transverse magnetic field and gravity field. Fusion Technol., 36: 247-262.

Patankar, S.V. and D.B. Spalding, 1970. Heat and mass transfer in boundary layers. 2nd Edn., Intertext, London

Patankar, S.V. and D.B. Spalding, 1972a. A calculation procedure for heat mass and momentum transfer in 3-dimensional parabolic flows. Intl. J. Heat Mass Transfer, 115: 1787-1803.

Patankar, S.V. and D.B. Spalding, 1972b. A computer modal for 3-dimensional flows in furnaces. Proc. 14th Symp. (Int.) on Combustion, the Combustion Inst., pp: 605.

Patankar, S.V. and D.B. Spalding, 1974a. A calculation procedure for the transient and steady state behavior of shell and tube heat exchanger. Chapter 7 in Heat Exchanger: Design and Theory Source Book, Hemisphere, Washington, DC.

Patankar, S.V. and D.B. Spalding, 1974b. Simultaneous predictions of flow pattern and radiation for 3-dimensional flames. Chap. 4 in Heat Transfer in Flames, Hemisphere, Washington, DC.

Patankar, S.V. and D.B. Spalding, 1978. Computer analysis of the 3-dimensional flow and heat transfer in stream generator. forsch. Ingenieurwes, pp: 44: 47.

Patankar, S.V., 1980. Numerical Heat Transfer and Fluid Flow. Hemisphere Publishing Corporation, New York.

Piet, S.J., 1986. Common views of potentially attractive fusion concept. Proc. 7th TopI. Mtg. Technology of Fusion Energy, Reno, Nevada.